Combustion and Flame 160 (2013) 2283–2290

Contents lists available at SciVerse ScienceDirect

Combustion and Flame

journal homepage: www.elsevier.com/locate/combustflame

Further study on the ignition delay times of propane–hydrogen–oxygen–argon mixtures: Effect of equivalence ratio

Chenglong Tang *, Xingjia Man, Liangjie Wei, Lun Pan, Zuohua Huang *

State Key Laboratory of Multiphase Flows in Power Engineering, Xi'an Jiaotong University, Xi'an 710049, People's Republic of China

ARTICLE INFO

Article history:
Received 24 January 2013
Received in revised form 22 March 2013
Accepted 12 May 2013
Available online 29 May 2013

Keywords:
Ignition delay times
Hydrogen fraction
Shock tube measurement
Equivalence ratio dependence
Chemical kinetic

ABSTRACT

Using a shock tube facility, measurements on ignition delay times of propane/hydrogen mixtures (hydrogen fraction X_{H2} is from 0% to 100%) were conducted at equivalence ratios of 0.5, 1.0 and 2.0. Results show that when X_{H2} is less than 70%, ignition delay time shows a strong Arrhenius temperature dependence, and the ignition delay time increases with the increase of equivalence ratio. When X_{H2} is larger than 95%, the ignition delay times do not retain an Arrhenius-like temperature dependence, and the effect of equivalence ratio is very weak when the hydrogen fraction is further increased. Numerical studies were made using two selected kinetic mechanisms and the results show that the predicted ignition delay times give a reasonable agreement with the measurements under all test conditions. Both measurements and predictions show that for mixtures with X_{H2} less than 70%, the ignition delay time is only moderately decreased with the increase of X_{H2}, indicating that hydrogen addition has a weak effect on the ignition enhancement. Sensitivity analysis reveals the key reactions that control the simulation of ignition delay time. Further investigation of the H-atom consumption is made to interpret the ignition delay time dependence on equivalence ratio and X_{H2}.

1. Introduction

Hydrogen has high reactivity and its combustion offers many advantages such as good lean burn stability, low minimum ignition energy and no greenhouse gas emissions. On the other hand, however, pure hydrogen fueled combustors are challenged by hydrogen's high knock tendency, high combustion temperature which leads to a high level of NOx emissions. The increasing consumption of fossil fuels and the consequent deterioration in atmospheric environment are leading the combustion community to find clean and renewable energy sources and to develop highly-efficient combustion techniques. Thus the investigation on hydrogen-blended hydrocarbon combustion is an area of current interest. Practically, studies on internal combustion engines showed that hydrogen addition could increase the brake thermal efficiency and reduce the green house gas emissions [1–3]. Studies of gas turbine combustors [4–6] showed that hydrogen addition could enhance lean burn stability, and reduces CO emission, without bringing the increase of NOx emissions.

Fundamentally, laminar flame speeds of hydrogen enriched methane or natural gas have been measured using the spherically expanding flame method [7–9], the stagnation flame method [10–12] and the heat flux method [13]. Ignition delay times of the hydrogen blended methane using shock tubes were also reported [14–16]. These experimental data are of merit for validating the small hydrocarbon kinetic mechanism, which is essential in the hierarchical structure of a kinetic model for hydrocarbons [17]. However, the investigation on hydrogen enriched higher hydrocarbons is still limited. The behaviors of spherically expanding flames of hydrogen enriched propane were characterized [18–22] and these studies showed that laminar flame speed increases a little at first, and then increases substantially with an increase in hydrogen fraction in the fuel blends. Additionally, hydrogen addition changes the flame front behavior through modifying the diffusional-thermal properties of the mixture. Recently, Tang et al. [23] measured the laminar flame speeds of hydrogen enriched butane by using the hydrogen addition parameter, R_H, defined by Yu et al. [10]. They found that laminar flame speed increases linearly with increasing R_H and this dependence is generalized to methane, propane, and ethene. There has been even less work on the ignition delay times of hydrogen enriched higher hydrocarbons. Lata and Misra [24] investigated the effect of hydrogen substitution on the ignition delay time in a dual fuel diesel engine. The ignition delay time was defined as the time interval between the start of fuel injection and the instant when the net heat release rate becomes zero. They stated that the ignition delay times of the mixtures were sensitive to the pre-ignition reaction rate and heat release rate. However, due to the complexity of combustion in engines, the ef-

* Corresponding authors. Fax: +86 29 82668789.
E-mail addresses: chenglongtang@mail.xjtu.edu.cn (C. Tang), zhhuang@mail.xjtu.edu.cn (Z. Huang).

0010-2180/$ - see front matter © 2013 The Combustion Institute. Published by Elsevier Inc. All rights reserved.
http://dx.doi.org/10.1016/j.combustflame.2013.05.012

Table 1
Compositions of the test mixture.

Mixtures	The mole fraction of C_3H_8 (%)	The mole fraction of H_2 (%)	The mole fraction of O_2 (%)	The mole fraction of Ar (%)
X_{H2} = 0				
ϕ = 0.5	0.514	0.000	5.142	94.344
1.0	1.008	0.000	5.038	93.954
2.0	1.937	0.000	4.843	93.220
X_{H2} = 70%				
ϕ = 0.5	0.403	0.940	4.968	93.689
1.0	0.765	1.784	4.715	92.737
2.0	1.388	3.238	4.279	91.096
X_{H2} = 95%				
ϕ = 0.5	0.158	3.005	4.586	92.252
1.0	0.281	5.334	4.071	90.314
2.0	0.459	8.712	3.324	87.505
X_{H2} = 100%				
ϕ = 0.5	0.000	4.339	4.339	91.322
1.0	0.000	7.394	3.697	88.908
2.0	0.000	11.413	2.853	85.734

fect of hydrogen addition is hard to be recognized and these ignition delay times data cannot be used for kinetic mechanism validation. Aggarwal et al. [25] numerically studied the effect of hydrogen addition on the ignition delay time of n-heptane/air mixtures by using several kinetic mechanisms and they found that the addition of hydrogen had a relatively small effect on the ignition of n-heptane/air mixture.

Previously the authors have reported ignition delay times of hydrogen/propane mixtures in argon diluted oxygen at an equivalence ratio of 0.5 and with hydrogen fractions ranging from 0% to 100% [26]. It is noted that the ignition delay time study on hydrogen/natural gas by Herzler and Naumann [15] indicates that equivalence ratio dependence varies with the hydrogen addition level, thus one objective of this study is to extend our previous study to different equivalence ratios in order to examine the ignition delay time response to mixture richness for different hydrogen addition levels. Furthermore, recently developed kinetic mechanisms [27,28] will be used to validate against the measured ignition delay times of the hydrogen enriched propane mixtures at different equivalence ratios. Finally, a kinetic analysis will be conducted to interpret the effect of equivalence ratio on different hydrogen addition level mixtures.

2. Experimental and numerical approaches

2.1. Experimental setup

The shock tube has a 2 m long driver section (driver gases: helium and nitrogen) and a 7.3 m long driven section with a diameter of 115 mm. The double diaphragms separate the driver and driven section before the experiment and the shock wave is generated by bursting the diaphragms. Depending on the magnitude of the reflected pressure, diaphragms of different thicknesses were selected. The driven section can be evacuated to pressure below 10^{-1} bar before the reactant mixture is added. Four fast-response sidewall pressure transducers (PCB 113B26) are located at fixed intervals (300 mm) along the end part of driven section. Three time counters (FLUKE, PM6690) with an uncertainty of 1 μs, are used to record the time interval between the instants of shock arrival at each pressure transducer location and the incident shock velocity is then correspondingly calculated. The velocity of the shock wave at the endwall is determined by extrapolating the shock velocity profile to the endwall. Typical attenuation rates of the incident shock are found to be less than 3%. On the endwall, another piezoelectric pressure transducer (PCB 113B03) was mounted to measure the pressure behind the reflected shock wave. Additionally, a quartz-glass window (60 mm thick) together with a 307.8 nm narrow band pass filter and a photomultiplier (Hamama-138 tsu, CR131) are mounted, through which the OH^* emission is captured. With the measured shock wave velocity, the temperature (T_5) behind the reflected shock wave is then calcu-

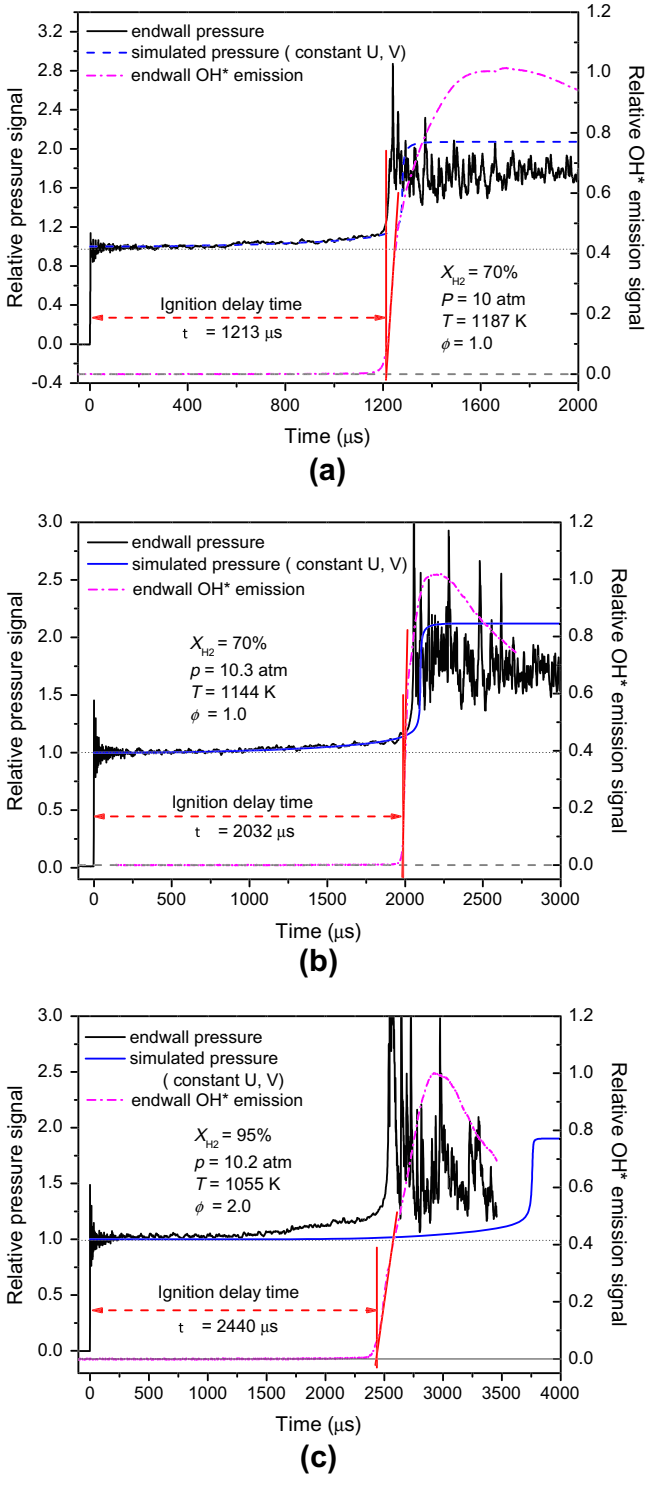

Fig. 1. Definition of ignition delay times, showing that the pressure rise before ignition is primarily sourced from the pre-ignition reaction and the facility dependent pressure rise is negligible for short ignition delay times.

Table 2
Correlation parameters for Eq. (1) for propane/hydrogen mixtures.

	$A \times 10^4$	α	β	E_a (kcal/mol)	R-square
X_{H2} = 0%	5.89 ± 0.26	0.556 ± 0.050	−0.473 ± 0.026	38.40 ± 0.98	0.979
X_{H2} = 70%	6.55 ± 0.29	0.661 ± 0.052	−0.487 ± 0.028	36.65 ± 0.89	0.977

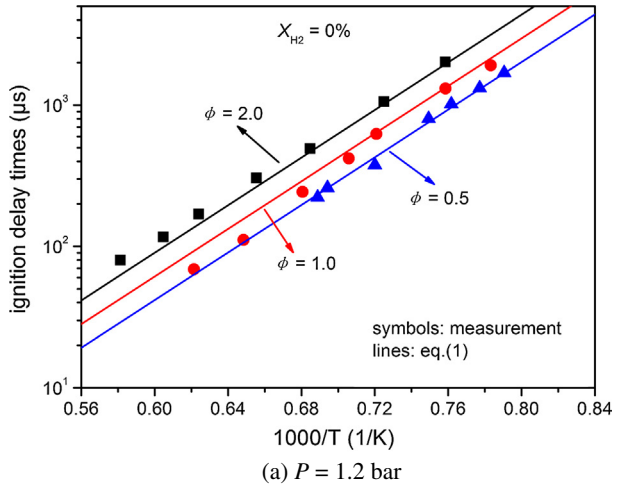

(a) P = 1.2 bar

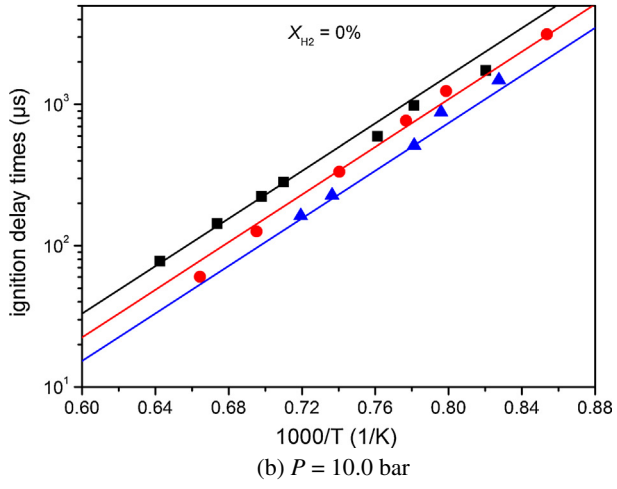

(b) P = 10.0 bar

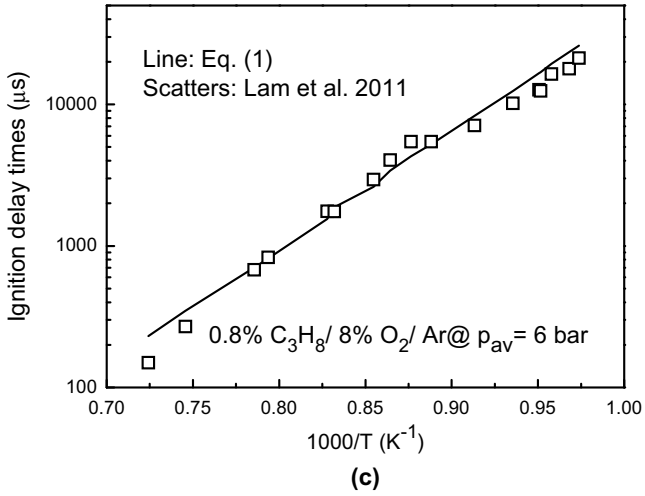

(c)

Fig. 2. Ignition delay times of pure propane at various equivalence ratios and pressures of (a) 1.2 bar, (b) 10.0 bar, and (c) 6 bar.

lated by using the chemical equilibrium program GasEq [29]. The uncertainty of T_5 is evaluated by using the same method as in Ref. [30] and typical error is around 40, 25 and 20 K, respectively for temperature and Mach number around (1500 K, 2.5), (1000 K, 2.1), and (900 K, 1.9). Consequently, the error in the measured ignition delay time is evaluated to be around 15%. Typical uncertainties in the ignition delay times and the temperatures are illustrated in Figs. 6 and 7.

The reactant mixtures are prepared separately in a 128 L stainless-steel tank according to the partial pressure of each gas component. After filling the tank, the mixtures were kept still over night to achieve perfect mixing. All the mixture compositions studied in this work are summarized in Table 1, where X_{H2} represents the fraction of hydrogen in the fuel blends, ϕ is equivalence ratio. Purities of hydrogen, oxygen and argon are all higher than 99.99%, and purity of propane is 99.9%.

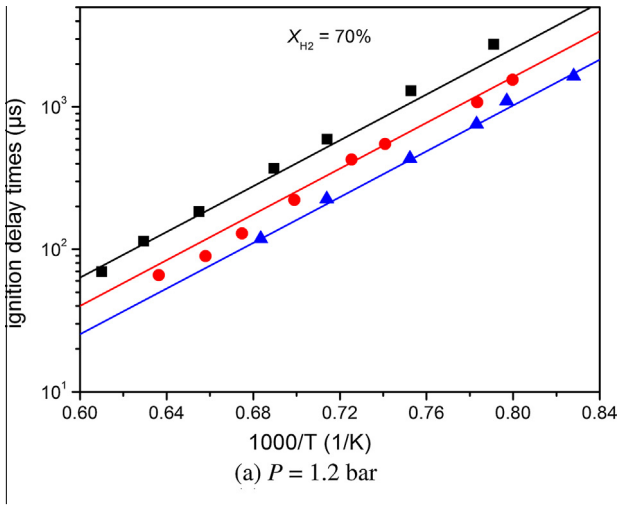

(a) P = 1.2 bar

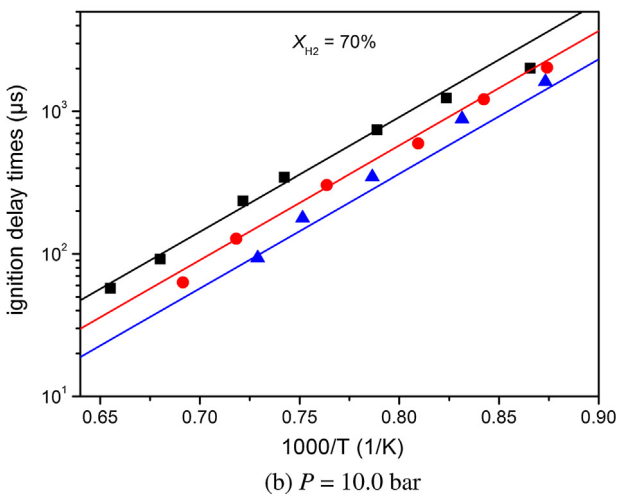

(b) P = 10.0 bar

Fig. 3. Ignition delay times of X_{H2} = 70% at various equivalence ratios and pressures of 1.2 and 10.0 bar.

2.2. Kinetic simulation

For numerical predictions, two kinetic mechanisms, NUI Mech [27] and USC Mech II [28] are used. The NUI Mech was developed in 2010 by Curran group for the natural gas kinetic modeling, in which 293 species and 1593 reactions are involved. The USC Mech II model, which includes 111 species and 784 reactions, was developed on the basis of oxidization of hydrogen and C1–C4 hydrocarbons by Wang's group. Both models have been extensively validated against the experimental data, such as laminar flame speeds [23] and ignition delay times [16,27] of methane. However, neither model has been validated against the ignition delay times of propane/hydrogen mixtures.

The SENKIN code in the CHEMKIN II package was used to calculate the ignition delay times of the hydrogen enriched propane mixtures by adopting the zero-dimensional and constant volume adiabatic model. The computational ignition delay time is defined as the time interval between zero and the moment of maximum rate of temperature rise (max dT/dt) in this study. The maximum OH rise rate definition was also tested, and no noticeable different in the computational results were found. In this study, the ignition delay times under all conditions are less than 2 ms.

The ignition delay time is defined as the time interval between the arrival of the shockwave at the endwall and the onset of the ignition. Figure 1a shows the typical endwall pressure and OH* emission profiles. It is seen that at $t = 0$, the shockwave arrived at the endwall. As time proceeded, there was no noticeable OH* emission signal until around 1213 μs where a steep increase in OH* emission signals was detected. Simultaneously, there was significant pressure increase at around 1213 μs. Thus the onset of ignition was recognized. It is noted that a certain pressure rise before ignition was observed. There are two sources for this pressure rise [31]: (a) the shock-tube facility effect; (b) heat release. The factor (a) depends on the dimension, the material and the texture of the shock tube, and the factor (b) arises from the reactions. In Fig. 1, we have compared the measured pressure (the black solid line) with the simulated pressure using the constant U, V assumption (the blue dash line). It is seen that for ignition delay times less than around 2 ms (Fig. 1a and b), the two lines almost overlap, thus the facility effect pressure rise is negligible. However, when the ignition delay times is large enough, as seen in Fig. 1c, the measured pressure is higher than the simulated ones, which indicates that the facility effect dp/dt should be considered for the ignition delay time calculation.

3. Results and discussion

3.1. Ignition delay times data: measurement and empirical correlation

Data of the ignition delay times under all test conditions are provided in the Supplementary material. Under some conditions, the ignition delay time exhibits a pseudo-Arrhenius behavior with

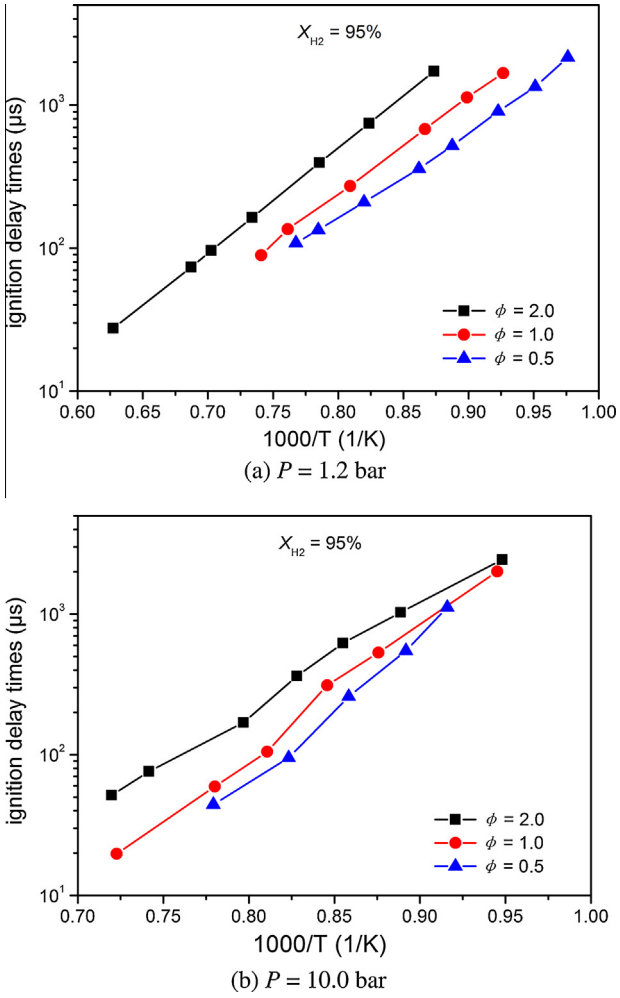

Fig. 4. Ignition delay times of X_{H2} = 95% at various equivalence ratios and pressures of 1.2 and 10.0 bar.

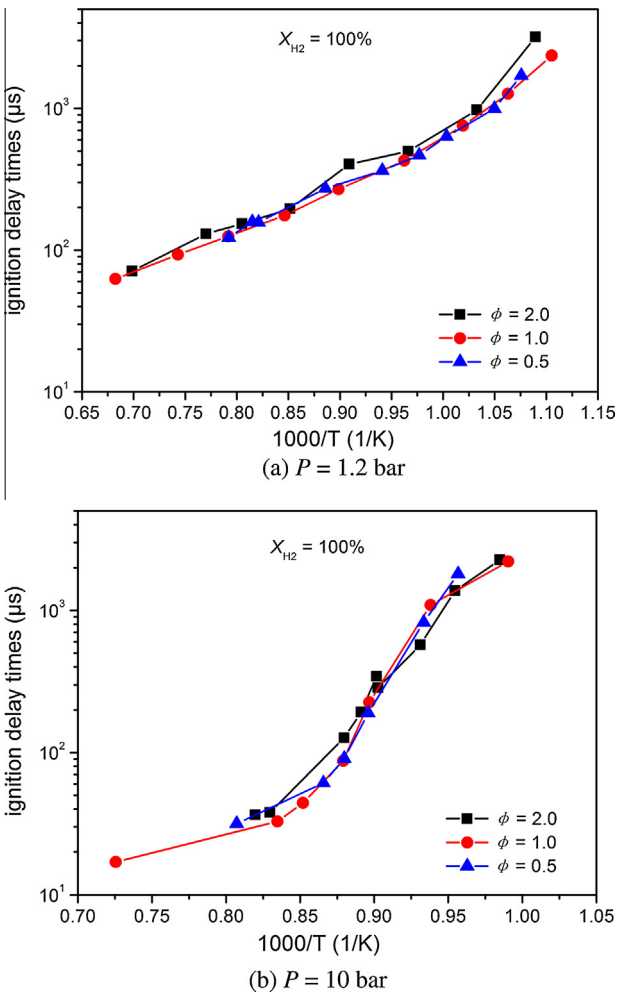

Fig. 5. Ignition delay times of pure hydrogen at various equivalence ratios and pressures of 1.2 and 10.0 bar.

respect to temperature, indicating the typical Arrhenius dependence of ignition delay time on temperature. The following empirical correlation is obtained using the multi-regression correlation,

$$\tau = A\phi^{\alpha}p^{\beta}\exp(E_a/RT) \quad (1)$$

The correlation parameters for each mixture condition is given in Table 2, where $R = 1.986 \times 10^{-3}$ kcal/(mole K) is universal gas constant, and E_a is global activation energy in kcal/mol, and τ is ignition delay time in microsecond. It should be noted that Eq. (1) is only applicable for empirically calculating the ignition delay times under the test conditions in this study. For the mixtures that do not exhibit the Arrhenius dependence of ignition delay time on temperature, only experimental data are provided and no correlations were provided.

Figure 2a gives the ignition delay times of pure propane ($X_{H2} = 0$) at equivalence ratios of 0.5, 1.0 and 2.0 and pressure of 1.2 bar. The ignition delay time exhibits a clear Arrhenius dependence on temperature at all equivalence ratios. Ignition delay time increases with the increase of equivalence ratio. Parallel lines of ignition delay time versus inverse temperature at different equivalence ratios are demonstrated, indicating that for no hydrogen addition case, the overall activation energy of different equivalence ratios are very equivalent, which is around 38.40 kcal/mol, as shown in Table 2. At higher pressure, as shown in Fig. 2b, similar behavior of the ignition delay time was observed: increasing the equivalence ratio has a decelerating effect on ignition. Figure 2c shows the Eq. (1) correlation with previous measurements form Lam et al. [32] for pure propane at an average pressure of 6 bar. It is seen that the Eq. (1) correlation agrees well with the measurements, which verifies the confidence of the present shock tube.

Figure 3 shows the ignition delay times for the fuel blend with high hydrogen addition ($X_{H2} = 70\%$). An Arrhenius temperature dependence of ignition delay times is still existed. Rich mixture gives longer ignition delay times than those of lean and stoichiometric mixtures. The overall activation energy is unchanged at different equivalence ratios for the fuel blend. The similarity of the ignition delay times of pure propane case and $X_{H2} = 70\%$ case indicate that the ignition of the fuel blend is primarily governed by the propane chemistry and even up to 70% hydrogen addition does not necessarily alter the ignition delay time dependence on the equivalence ratio. However, the derived overall activation energy is decreased to 36.65 kcal/mol. When the hydrogen fraction is further increased, as shown in Fig. 4a, the logarithmic ignition delay time no longer retains the perfect linear relation with the inverse temperature. This phenomenon is more significant at 10 bar pressure. Thus the global correlation of the ignition delay time as Eq. (1) is not available. Similarly, the rich mixture gives longer ignition delay times than those of lean and stoichiometric mixtures. Figure 5 shows the ignition delay times versus temperature for the pure hydrogen mixture ($X_{H2} = 100\%$). The influence of equivalence ratio on the ignition delay time is very weak. The effect of equivalence

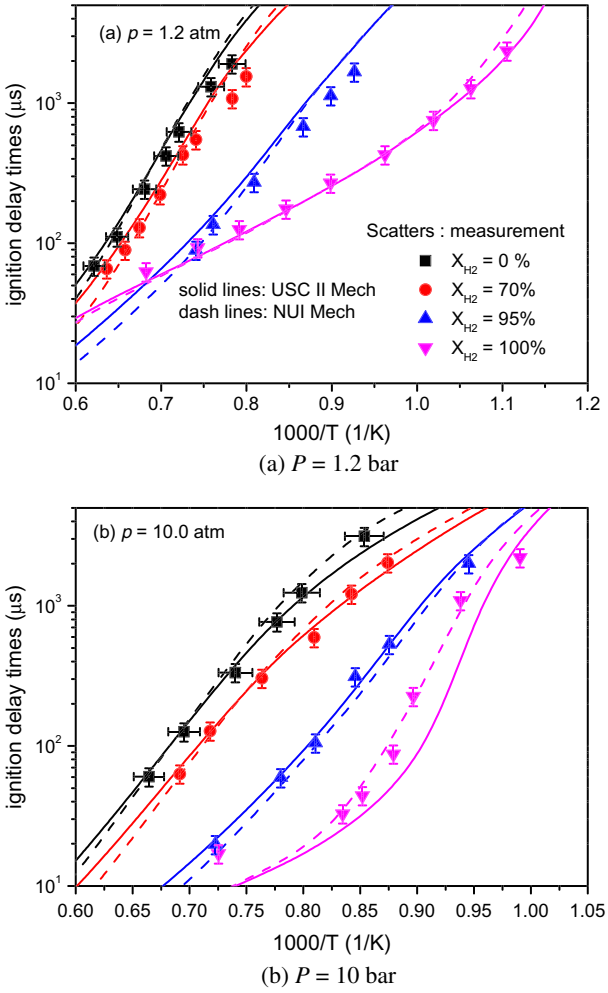

Fig. 6. Measured and simulated ignition delay times of propane–hydrogen blends at equivalence ratio of 1.0 and pressures of 1.2 and 10.0 bar.

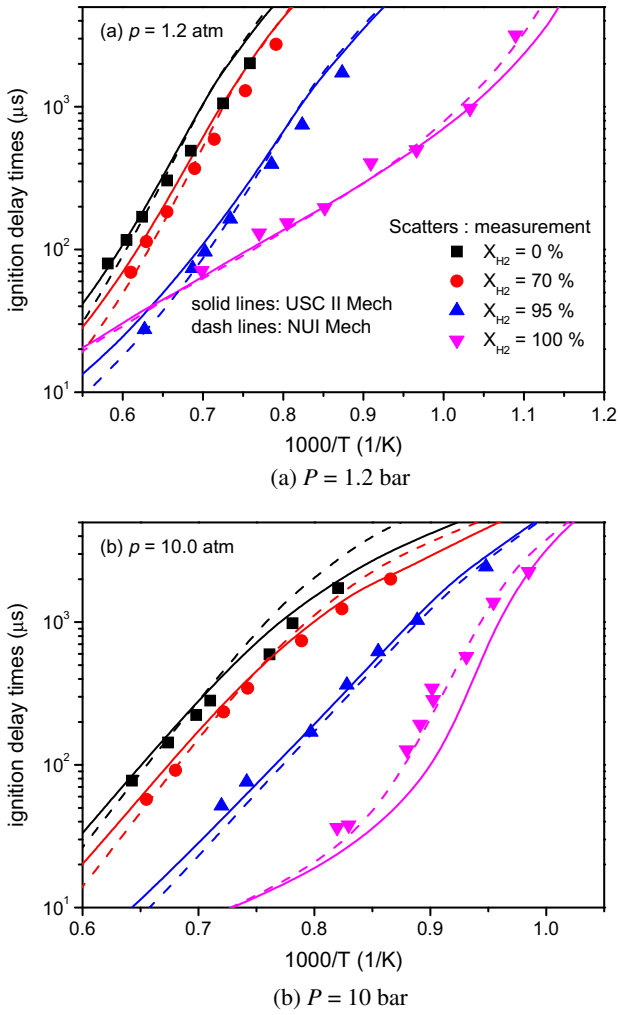

Fig. 7. Measured and simulated ignition delay times of propane–hydrogen blends at equivalence ratio of 2.0 and pressures of 1.2 and 10.0 bar.

ratio on the ignition delay times at various hydrogen additions will be discussed later through the kinetic analysis.

3.2. Numerical predictions

Figures 6 and 7 give the comparisons between the measured and model predicted ignition delay times. It is noted that for ignition delay times longer than around 2 ms, the constant *U*, *V* assumption should be revised because the facility dependent pressure rise, as discussed in the end of Section 2.2. The facility dependent pressure rise was found to have an average of 2.5%/ms and was included in the computations when the ignition delay time is longer than 2 ms. Generally, the two models predict well the ignition delay times of pure hydrogen. Specifically, for the stoichiometric mixture at 1.2 bar, both models slightly over-predict the ignition delay times for pure propane, and for propane–hydrogen fuel blends of X_{H2} = 70% and X_{H2} = 95% at relatively lower temperatures as shown in Fig. 6a. For pure hydrogen (X_{H2} = 100%), USC Mech II yields excellent agreement with the measurements. At pressure of 10.0 bar, as shown in Fig. 6b, USC Mech II gives perfect prediction on the ignition delay times for pure propane, propane–hydrogen fuel blends of X_{H2} = 70% and X_{H2} = 95%, while it underpredicts the ignition delay times for pure hydrogen. The NUI Mech slightly over-predict the ignition delay times at relatively higher temperatures for pure propane, propane–hydrogen fuel blends of X_{H2} = 70% and X_{H2} = 95%, but it gives perfect predictions for pure hydrogen. For rich mixture (equivalence ratio of 2.0), as shown in Fig. 7, both models slightly over-predict the ignition delay times for pure propane, propane–hydrogen fuel blends of X_{H2} = 70% and X_{H2} = 95% at relatively lower temperatures, but excellent predictions for pure hydrogen at 1.2 bar. The USC Mech II under-predicts the ignition delay times at 10.0 bar. For the fuel blends with X_{H2} less than 95%, the NUI Mech predicted ignition delay time intersects with the USC Mech II predicted ones and the intersection point shifts to the lower temperature as X_{H2} is increased. Both model predictions and measurements show that for the fuel blends with X_{H2} less than 70%, the ignition delay times exhibits the Arrhenius dependence on temperature, and ignition delay times is only moderately decreased even 70% hydrogen addition. However, when X_{H2} is larger than 95%, the ignition delay time is significantly decreased with increasing X_{H2} and it does not retain the Arrhenius dependence on temperature.

3.3. Chemical kinetic interpretations on the effect of equivalence ratio

The ignition delay time dependence on the equivalence ratio for different hydrogen fraction mixtures as shown in Figs. 2–5 should be ascribed to the different ignition chemistry of the mixtures and

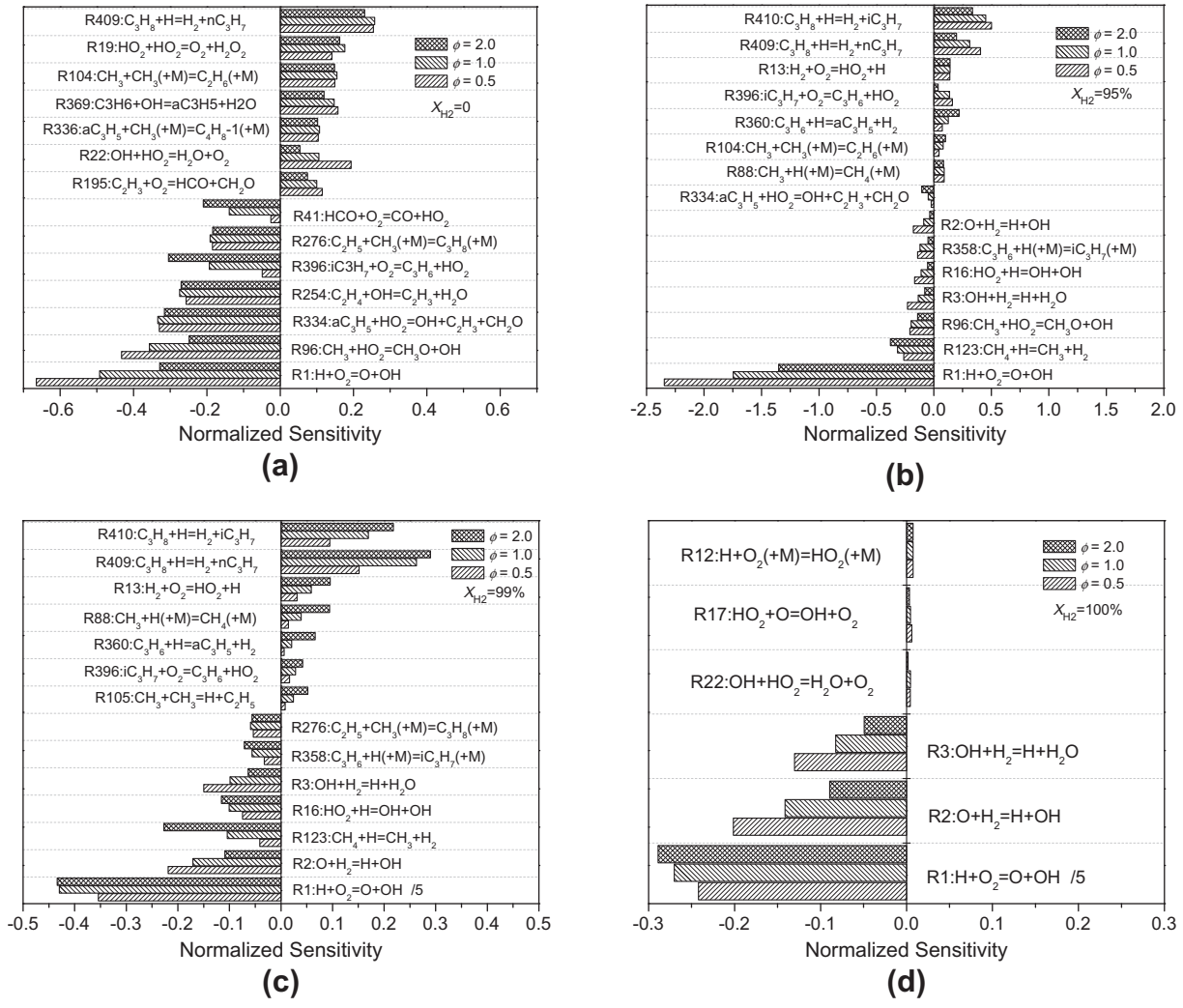

Fig. 8. Sensitivity coefficients as a function of equivalence ratio for different X_{H2} mixtures at 1200 K and 10.0 bar.

we note that with the increase of X_{H2}, the ignition of the mixture resembles more and more that of the pure hydrogen system.

3.3.1. Sensitivity analysis

To interpret the ignition delay time dependence on equivalence ratio at various hydrogen additions, the sensitivity analysis of reactions is performed,

$$S = \frac{\tau(2.0k_i) - \tau(0.5k_i)}{1.5\tau(k_i)} \quad (2)$$

where τ is ignition delay time of the mixtures and k_i is rate constant of the ith reaction, and S is the normalized sensitivity coefficient. Positive sensitivity coefficients indicate an increase in ignition delay times as reaction rate is increased and the corresponding reaction is the ignition inhibited reaction and vice versa. Through sensitivity analysis, the reactions that most profoundly affect the ignition delay time predictions can be identified. It is noted that sensitivity coefficients based on both the NUI Mech and USC Mech II were obtained. For most of the mixtures, the results are similar, indicating that the dominant reactions for the ignition of the mixtures in these two models are similar.

Figure 8 presents the reactions with the highest normalized sensitivity coefficients of different hydrogen additions at various equivalence ratios and pressure of 10.0 bar and temperature of 1200 K. For the propane–hydrogen fuel blends with $X_{H2} \leqslant 95\%$, as shown in Fig. 8a and b, the reactions with the highest positive sensitivity coefficients (most inhibiting reactions) at lean, stoichiometric and rich mixtures are the H-abstraction reactions of propane, $C_3H_8 + H = H_2 + nC_3H_7$ (R409) and $C_3H_8 + H = H_2 + iC_3H_7$ (R410). These two reactions consume the H radical and form the stable hydrogen molecule, leading to the reduction of system reactivity. The most promoting reaction is the chain branching reaction $H + O_2 = OH + O$ (R1). Additionally, for a given X_{H2}, the sensitivity coefficients of these three reactions are generally decreased with the increase of equivalence ratio. For the propane–hydrogen fuel blend with $X_{H2} = 99\%$, as shown in Fig. 8c, the similar dominant reactions are presented. The most ignition promoting reaction is still R1 and the most inhibiting reactions are still R410 and R409, however, their sensitivity coefficients dependence on equivalence ratio is opposite to that of $X_{H2} = 95\%$ fuel blend. For pure hydrogen, as shown in Fig. 6d, the ignition delay time is dominated by R1 and the ignition inhibiting reactions have very small positive sensitivity coefficients.

For small X_{H2} mixtures, with the increase of the equivalence ratio, the H-scavenging reactions R409 and R410 are favored because of the increased C_3H_8 concentration (as shown in Table 1), leading

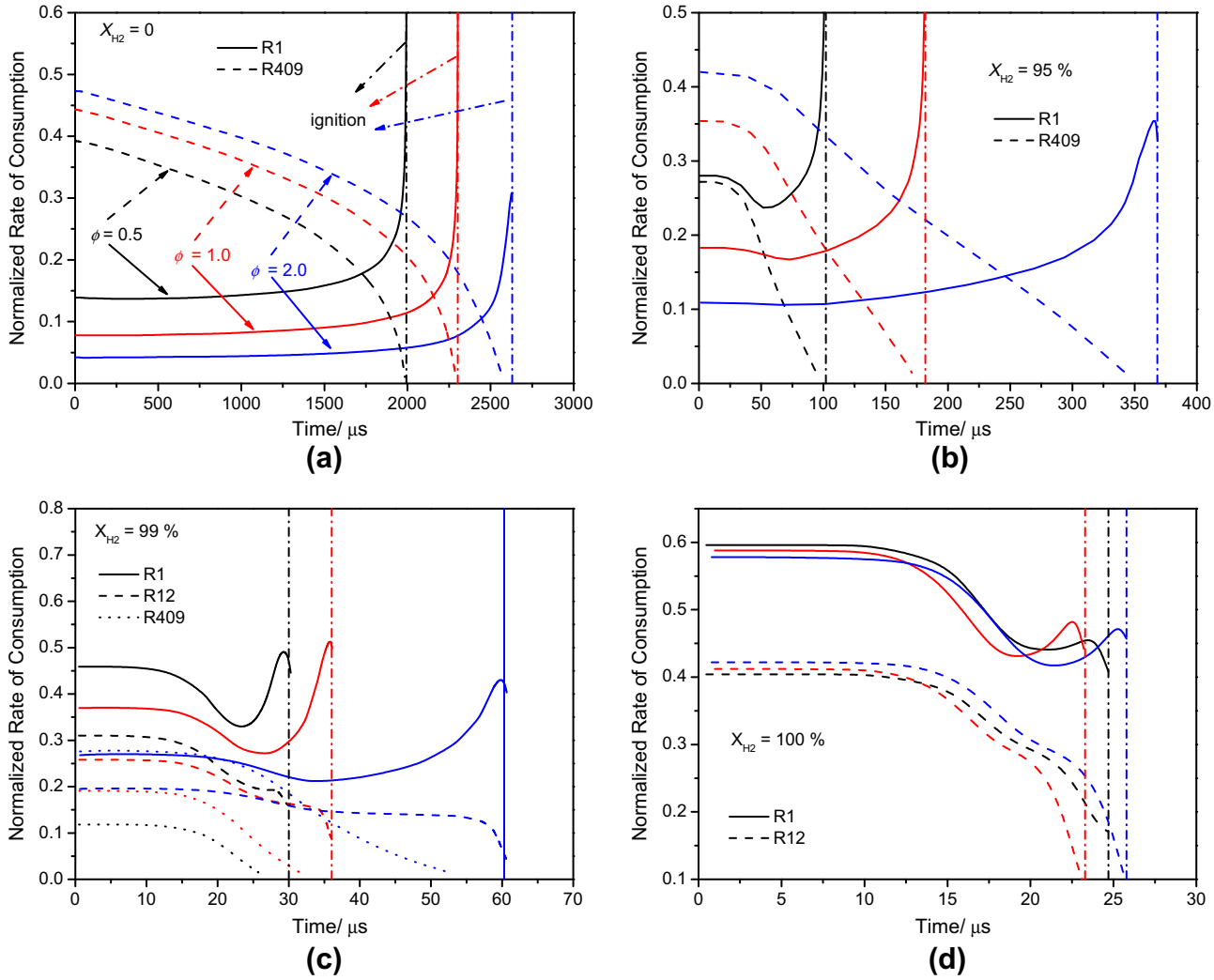

Fig. 9. Reactions with the highest H radical consumption rates at various equivalence ratios and hydrogen addition at 1200 K and 10.0 bar. The consumption rate is normalized through the total rate of consumption. The black, red and blue lines respectively represent the equivalence ratios of 0.5, 1.0, and 2.0. (For interpretation of the references to color in this figure legend, the reader is referred to the web version of this article.)

to an increased ignition delay time. As also shown in Table 1, for higher X_{H2} mixtures, the C_3H_8 concentration increase with increasing equivalence ratio becomes progressively less, while the concentration of H_2 increases more strongly, thus the mixture ignition behavior resembles more and more that of pure hydrogen. Consequently, the ignition delay time is becoming less and less dependent on the equivalence ratio, as shown in Figs. 2–5.

3.3.2. Consumption of H atoms

To further understand the controlling reactions in the ignition chemistry and the effect of equivalence ratio on the ignition delay time at various hydrogen additions, the rate of consumption of H atoms as a function of time at 10 bar before ignition is provided in Fig. 9. For the pure propane, as shown in Fig. 9a, the H abstraction reaction of propane (R409) initially dominates the H consumption and its contribution reduces gradually. The ignition delay times at three equivalence ratios are in the range between 2000 and 2600 μs. At $\phi = 0.5$, ignition occurs at around 2000 μs where there is a dramatic increase in H atom consumption through reaction R1. With the increase of equivalence ratio, the consumption rate of H atom from reactions R1 and R409 decrease. Similarly, for the mixture with $X_{H2} = 95\%$, as shown in Fig. 9b, the dominant consumption reactions of H atom are still the reactions R1 and R409 and their contributions are decreased with the increase of equivalence ratio. The ignition delay times of these propane–hydrogen fuel blends are between 100 and 400 μs. Furthermore, at $\phi = 1.0$ and 2.0, the rate of consumption from R409 are still initially higher than that of R1, but the contribution of R1 quickly overtakes R409 as time proceeds. At $\phi = 0.5$, R1 becomes more effective than R409 in H radical consumption during the whole ignition process. Figure 9a and b demonstrated that the dominance of the promoting reaction R1 which leads to fast ignition and the dominance of the inhibiting effect of R409 which leads to long ignition delay times.

For even higher hydrogen addition ($X_{H2} = 99\%$) at this pressure, as shown in Fig. 9c, the ignition delay times at various equivalence ratios are between 30 and 60 μs. The rate of consumption from reaction R1 becomes the largest at $\phi = 0.5$ and 1.0, while at $\phi = 2.0$, another ignition inhibiting reaction $H + O_2 + M = HO_2 + M$ (R12) becomes effective and its rate of consumption is comparable to that of R409. The contribution from R1 is still sensitive to equivalence ratio. However, the relative difference between the rates of consumption is significantly smaller, compared to the mixtures with smaller X_{H2} in Fig. 9a and b. For pure hydrogen, as shown in Fig. 9d, the ignition delay times at the three equivalence ratios are around 25 μs. Reaction R1 becomes the dominant consumption reaction of H radical at the three equivalence ratios and its rate of consumption is much higher than that of the ignition retarding reaction R12. Furthermore, the rate of H consumption is insensitive to the equivalence ratio, which explains the negligible ignition delay time dependence on equivalence ratio as shown in Fig. 5.

4. Concluding remarks

Further investigation on the ignition delay times of propane–hydrogen fuel blends in argon diluted oxygen were conducted, with the emphasis on the effect of equivalence ratio. The measured and numerically predicted ignition delay times agree well under all test conditions in this work. When hydrogen fraction is less than 70%, the ignition delay time exhibits a strong Arrhenius temperature dependence. With the increase of equivalence ratio, the ignition delay time is significantly increased. When hydrogen fraction is larger than 95%, there is no Arrhenius temperature dependence any more, and the equivalence ratio has very weak effect on the ignition delay times. Chemical kinetic analysis reveals that the ignition phenomenon of the different equivalence ratio mixtures is controlled by the competition of the propane chemistry through R409 and R410 which leads to long ignition delay times and clear equivalence ratio dependence and the hydrogen chemistry through R1 which leads to short ignition delay times and almost no equivalence ratio dependence.

Acknowledgments

This work is supported by the National Natural Science Foundation of China (51206131, 51136005, 51121092), and the National Basic Research Program (2013CB228406). Authors also appreciate the funding support from the Fundamental Research Funds for the Central Universities.

Appendix A. Supplementary material

Supplementary data associated with this article can be found, in the online version, at http://dx.doi.org/10.1016/j.combustflame.2013.05.012.

References

[1] F. Ma, Y. Wang, Int. J. Hydrogen Energy 33 (2008) 1416–1424.
[2] F. Ma, Y. Wang, H. Liu, Y. Li, J. Wang, S. Zhao, Int. J. Hydrogen Energy 32 (2007) 5067–5075.
[3] C.D. Rakopoulos, D.C. Kyritsis, Int. J. Hydrogen Energy 31 (2006) 1384–1393.
[4] P. Chiesa, G. Lozza, L. Mazzocchi, J. Eng. Gas Turbines Power 127 (2005) 73–80.
[5] R.W. Schefer, D.M. Wicksall, A.K. Agrawal, Proc. Combust. Inst. 29 (2002) 843–851.
[6] P. Strakey, T. Sidwell, J. Ontko, Proc. Combust. Inst. 31 (2007) 3173–3780.
[7] Z.H. Huang, Y. Zhang, K. Zeng, B. Liu, Q. Wang, D.M. Jiang, Combust. Flame 146 (2006) 302–311.
[8] F. Halter, C. Chauveau, N. Djebaïli-Chaumeix, I. Gökalp, Proc. Combust. Inst. 30 (2005) 201–208.
[9] E.J. Hu, Z.H. Huang, J.J. He, C. Jin, J.J. Zheng, Int. J. Hydrogen Energy 34 (2009) 4876–4888.
[10] G. Yu, C.K. Law, C.K. Wu, Combust. Flame 63 (1986) 339–347.
[11] J.Y. Ren, W. Qin, F.N. Egolfopoulos, T.T. Tsotsis, Combust. Flame 124 (2001) 717–720.
[12] C.M. Vagelopoulos, F.N. Egolfopoulos, Proc. Combust. Inst. 25 (1994) 1317–1323.
[13] F.H.V. Coppens, J. De Ruyck, A.A. Konnov, Combust. Flame 149 (2007) 409–417.
[14] J. Huang, W.K. Bushe, P.G. Hill, S.R. Munshi, Int. J. Chem. Kinet. 38 (2006) 221–233.
[15] J. Herzler, C. Naumann, Proc. Combust. Inst. 32 (2009) 213–220.
[16] Y. Zhang, Z. Huang, L. Wei, J. Zhang, C.K. Law, Combust. Flame 159 (2012) 918–931.
[17] C.K. Westbrook, F.L. Dryer, Symp. (Int) Combust. 18 (1981) 749–767.
[18] B.E. Milton, J.C. Keck, Combust. Flame 58 (1984) 13–22.
[19] C.K. Law, O.C. Kwon, Int. J. Hydrogen Energy 29 (2004) 867–879.
[20] C.K. Law, G. Jomaas, J.K. Bechtold, Proc. Combust. Inst. 30 (2005) 159–167.
[21] C.L. Tang, J.J. He, Z.H. Huang, C. Jin, J.H. Wang, X.B. Wang, H.Y. Miao, Int. J. Hydrogen Energy 33 (2008) 7274–7285.
[22] C.L. Tang, Z.H. Huang, C. Jin, J.J. He, J.H. Wang, X.B. Wang, H.Y. Miao, Int. J. Hydrogen Energy 33 (2008) 4906–4914.
[23] C.L. Tang, Z.H. Huang, C.K. Law, Proc. Combust. Inst. 33 (2011) 921–928.
[24] D.B. Lata, A. Misra, Int. J. Hydrogen Energy 36 (2011) 3746–3756.
[25] S.K. Aggarwal, O. Awomolo, K. Akber, Int. J. Hydrogen Energy 36 (2011) 15392–15402.
[26] X.J. Man, C.L. Tang, L. Wei, L. Pan, Z.H. Huang, Int. J. Hydrogen Energy 38 (2013) 2523–2530.
[27] M. Ó Conaire, H.J. Curran, J.M. Simmie, W.J. Pitz, C.K. Westbrook, Int. J. Chem. Kinet. 36 (2004) 603–622.
[28] H. Wang, X.Q. You, A.V. Joshi, S.G. Davis, A. Laskin, F. Egolfopoulos, C.K. Law, USC Mech Version II. High-temperature combustion reaction model of H2/CO/C1–C4 compounds. <http://ignis.usc.edu/USC_Mech_II.htm>, May 2007.
[29] A chemical equilibrium program for windows. <http://www.c.morley.dsl.pipex.com>.
[30] E.L. Petersen, M.J.A. Rickard, M.W. Crofton, E.D. Abbey, M.J. Traum, D.M. Kalitan, Meas. Sci. Technol. 16 (2005) 1716–1729.
[31] G.A. Pang, D.F. Davidson, R.K. Hanson, Proc. Combust. Inst. 32 (2009) 181–188.
[32] K.Y. Lam, Z. Hong, D.F. Davidson, R.K. Hanson, Proc. Combust. Inst. 33 (2011) 251–258.